

## Nano-structural, Electrical and Mechanical Characterization of Zirconium Oxide Thin Films as a Function of Annealing Temperature and Time

K. Khojier<sup>1,\*</sup>, S. Sarshar<sup>2,†</sup>, F. Jafari<sup>2,‡</sup>, A. Borzou<sup>1,§</sup>

<sup>1</sup> Department of physics, Chalous branch, Islamic Azad University, Chalous, Iran

<sup>2</sup> Department of physics, Faculty of sciences, Central Tehran branch, Islamic Azad University, Tehran, Iran

(Received 07 May 2013; published online 30 August 2013)

Zr thin films were deposited by DC magnetron sputtering technique on Si substrate and then post-annealed at different temperatures (150-750 °C in steps of 150 °C) and times (60 and 180 min) with flow of oxygen. X-ray diffraction (XRD) method was used for study of crystallographic structure. These results showed an orthorhombic structure for annealed films at 150 °C and a mixed structure of monoclinic and tetragonal for annealed films at higher temperatures (300-750 °C). XRD result also showed that an increase in annealing temperature and time caused increasing of crystalline size. EDAX and AFM techniques were employed for investigation of chemical composition and surface morphology of samples, respectively. The results showed a granular structure for all samples, while the O / Zr ratio, grains size and surface roughness were increased with increasing of annealing temperature and time. A two probe instrument was used for electrical properties investigation, while hardness of films was measured by nano-indentation test. These results showed that increasing of annealing temperature and time caused increasing of electrical resistance and decreasing of hardness in the films.

**Keywords:** Zirconium oxide, Thin film, Post-annealing, Nano-structure, Hardness, Electrical resistance.

PACS numbers: 64.46.Hk, 61.05.Cp, 62.20.Qp, 73.61.At

### 1. INTRODUCTION

Physical properties of nano-materials have been a subject of intense scrutiny over the past two decades because of the scientific and technological interest on the preparation method and nanostructure dependence of these properties [1-4]. Zirconia (ZrO<sub>2</sub>) is one of these materials that especially in the thin film form is very attractive. ZrO<sub>2</sub> has been applied at thermal barrier coatings [5], optical filters and laser mirrors [6], alternative gate dielectrics in microelectronics [7, 8], a buffer layer for a high  $T_c$  ceramic superconductor on Si [9], high temperature oxygen separation [10], oxygen sensors [11] and fuel cells [12] due to its heat resistance, low thermal conductivity, a relative high dielectric constant, high refractive index, high transparency in the visible and near-infrared region [13, 14]. In all these practical applications, the preparation method, control of growth, crystal structure, chemical composition, and electronic properties of ZrO<sub>2</sub> thin films are very important. Hence, characterization of structural, electrical, mechanical and optical properties of Zirconia thin films prepared using different deposition techniques and correlation between nano-structure and different properties of these films play an important role in their technical applications. Many researchers have been reported on investigation of different properties of ZrO<sub>2</sub> thin films prepared by different methods including thermal annealing [15, 16], sputtering [17, 18], reactive sputtering [19, 20], Chemical Vapor Deposition [21], electron beam evaporation [22], and sol-gel processing [23].

In this work, in order to more deeply understand

the effect of annealing conditions on the Zr thin films, we have prepared the Zirconium oxide thin films by post-annealing of Zr / Si films at different temperatures and times, and studied the influence of these variables on crystallographic structure, surface morphology, chemical composition and electrical and mechanical properties of these layers.

### 2. EXPERIMENTAL DETAIL

Conventionally polished silicon (Si (400),  $n$ -type) with dimensions of 20 × 20 mm<sup>2</sup> were used as a substrate. The substrates were cleaned with acetone and ethanol in ultrasound cleaner for several minutes and were dried by argon gas flow. Zr thin films of 90 nm thickness were deposited by means of DC magnetron sputtering system using a circular sputtering target (99.998 % purity) of 76 mm diameter and 1 mm thickness. The target to substrate distance was 10 cm. A continuously variable DC power supply of 600 V and 150 mA was used as a power source for sputtering. The thickness and deposition rate of the Zr films were checked in situ using a quartz crystal monitor (6 MHz gold, Inficon Company, USA) located near the substrate during the sputtering process. Zirconium thin films were deposited at a deposition rate of 9 Å/s. The base pressure was 4 × 10<sup>-5</sup> mbar, achieved with a diffusion pump coupled with a rotary pump that was changed to 2.8 × 10<sup>-3</sup> mbar after presence of Argon. The purity of argon gas in this work was 99.998 % and controlled by mass flow controller. Post-annealing of Zr / Si films were performed by a tube furnace at five

\* [khojier@iauc.ac.ir](mailto:khojier@iauc.ac.ir)

† [soheilasarshar@yahoo.com](mailto:soheilasarshar@yahoo.com)

‡ [Asalj1364@gmail.com](mailto:Asalj1364@gmail.com)

§ [farshadbr@yahoo.com](mailto:farshadbr@yahoo.com)

different temperatures (150 to 750 °C in steps of 150 °C) with flow of oxygen (purity of 99.98 %) at 200 sccm (standard cubic centimeter per minute). Two annealing times of 60 and 180 min were used. The samples were reached the selected annealing temperature with a thermal gradient of 5 degree/min, and then gradually cooled down to room temperature. The details of the samples produced in this work are given in Table 1. Nanostructure and crystallographic orientation of the samples were obtained using a Philips XRD X'pert MPD Diffractometer (Cu K $\alpha$  radiation, 40 kV and 30 mA) with a step size of 0.02° and count time of 1 s per step. A Field Emission Scanning Electron Microscope FESEM (model: CamScan MV2300, Czech & England) and an Atomic Force Microscope (Auto probe PC, Park Scientific Instrument, USA) were also employed for investigation of chemical composition and surface morphology, respectively. The electrical resistance of films was also measured by two probe instrument with an excitation wavelength at 320 nm, while films hardness was measured by nano-indentation test.

### 3. RESULT AND DISCUSSION

Fig. 1 shows X-ray diffraction patterns of Zr / Si thin films annealed at different temperature for 60 min. XRD pattern of annealed sample at 150 °C shows two peaks at 31.91° and 34.25° can be related to ZrO<sub>2</sub> (012) and ZrO<sub>2</sub> (111) diffraction lines of orthorhombic phase (with reference to JCPDS Card No.: 33-1483, and 2 $\theta$  31.889° and 34.222°). By increasing of annealing temperature to 300 °C, mentioned peaks of orthorhombic phase are omitted and three new peaks are observed at 28.05°, 29.81°, and 34.23°. These peaks can be attributed to ZrO<sub>2</sub> (111) crystallographic orientation of monoclinic phase (with reference to JCPDS Card No.: 05-0543, and 2 $\theta$  28.036°), ZrO<sub>2</sub> (101) crystallographic orientation of tetragonal phase (with reference to JCPDS Card No.: 24-1164, and 2 $\theta$  29.807°), and ZrO<sub>2</sub> (002) crystallographic orientation of monoclinic phase (with reference to JCPDS Card No.: 05-0543, and 2 $\theta$  34.195°), respectively. With increasing of annealing temperature to the higher temperatures (450, 600 and 750 °C) don't observe any new peaks. On the other hand, it can be concluded that the annealing temperature (in the range of 300-750 °C) have little influence on the structure of ZrO<sub>2</sub> films. The above mentioned behavior was also observed for annealed samples at higher annealing time (i.e., samples S6-S10). The XRD results detail of all samples are given in Table 1. It can be seen in column 4 of Table 1, that the position of all diffraction lines are shifted to higher diffraction angles relative to that of powder sample with increasing the annealing temperature. In addition those samples annealed at higher time (i.e. 180 min) show larger shift than those annealed at 60 min. These behaviors can be related to increasing of tensile stress by increasing of annealing temperature and time. The tensile stress can be also attributed to higher thermal expansion coefficient of ZrO<sub>2</sub> to Si that increases at higher annealing temperatures and time.

In order to obtain the crystalline size (coherently

diffracting domains) of the samples we used the Scherrer relation [24]:

$$D = \frac{k\lambda}{B \cos \theta}$$

where,  $\lambda$  is the wavelength of X-ray,  $\theta$  is the Bragg angle, and  $k$  is a dimensionless constant which is related to the shape and distribution of crystallites [25] (usually taken as unity). For obtaining the value for, we used the usual procedure of full width at half maximum (FWHM) measurement technique [26], therefore:

$$B = (W_0^2 - W_i^2)^{1/2}$$

where,  $W_0$  is the FWHM of the sample and  $W_i$  is the FWHM of stress free sample (standard SiO<sub>2</sub> single crystal sample). The calculated crystalline size,  $D$  obtained from the above procedure is given in column 5 of Table 1. This result shows that the increasing of annealing temperature and time cause the increasing of crystalline size in these films. This behavior may be due to high annealing temperature / more annealing time that provides energy of film atoms to enhance mobility. Increasing of mobility can also increases the coalescence and decreases the defects and cause the improvement of pores and quality of ZrO<sub>2</sub> films.

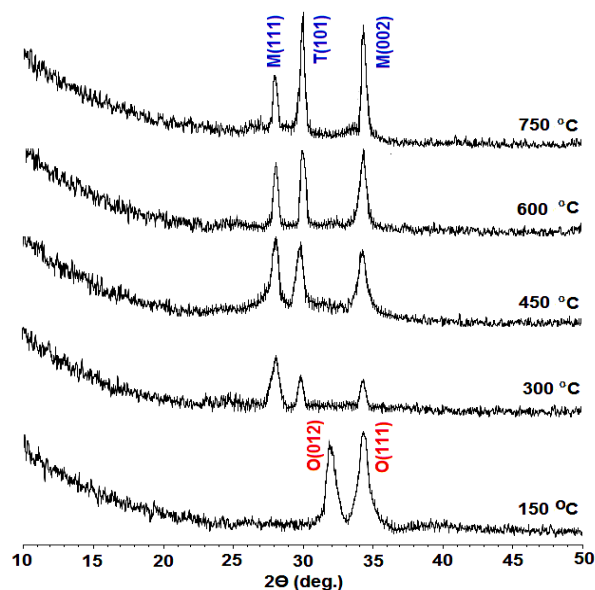


Fig. 1 – XRD patterns of Zr / Si thin films annealed at different temperatures for 60 min

3D AFM images of selected samples (annealed at different temperatures for 60 min) are shown in Fig. 2. The grains size (calculated by JMicrovision code from 2D AFM images) and surface roughness of all samples are plotted in Fig. 3 and 4, respectively. These results show that an increase in annealing temperature and time caused increasing grains size (consistent with XRD results) and surface roughness. Increasing of surface roughness can be related the increasing of grains size as mentioned before.

Table 1 – Detail of XRD analysis

	$T_i$ (°C)	$T_i$ (min)	$2\theta$ (deg.), (hkl)	$D_i$ (nm)
S1	150	60	31.89 / 34.23 O(012) / O(112)	33 / 37
S2	300	60	28.05 / 29.81 / 34.21 M(111) / T(101) / M(002)	61 / 65 / 64
S3	450	60	28.07 / 29.83 / 34.23 M(111) / T(101) / M(002)	83 / 81 / 87
S4	600	60	28.07 / 29.83 / 34.25 M(111) / T(101) / M(002)	97 / 95 / 102
S5	750	60	28.09 / 29.85 / 34.27 M(111) / T(101) / M(002)	133 / 159 / 151
S6	150	180	39.91 / 34.25 O(012) / O(112)	42 / 46
S7	300	180	28.07 / 29.83 / 34.21 M(111) / T(101) / M(002)	64 / 68 / 71
S8	450	180	28.09 / 29.85 / 34.23 M(111) / T(101) / M(002)	89 / 88 / 93
S9	600	180	28.09 / 29.87 / 34.27 M(111) / T(101) / M(002)	107 / 110 / 115
S10	750	180	28.09 / 29.87 / 34.29 M(111) / T(101) / M(002)	147 / 162 / 157

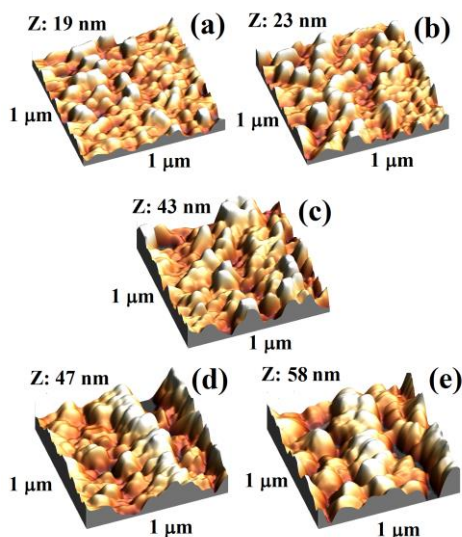


Fig. 2 – AFM images of Zr / Si thin films annealed at different temperatures for 60 min

The chemical composition of films was investigated by EDAX analysis. The results obtained from this analysis are shown in Fig. 5. These results show that ratio of O / Zr increases with increasing of annealing temperature and time. On the other hand, increasing of annealing temperature in the range of 150-750 °C, and annealing time improve the oxidation process.

Variation of electrical resistance of Zirconium oxide thin films obtained from two probe instrument for selected samples (annealed for 60 min) is shown in Fig. 6. The result shows that an increase in annealing temperature results increasing of films electrical resistance. It can be due to the increasing of oxygen vacancies in films body with increasing of annealing temperature.

Detail of hardness values of films is shown in Fig. 7. It can be seen that films hardness decreases with increasing of annealing temperature and time. This reduction can be related to increasing of crystalline size and surface roughness with annealing temperature and time (according to XRD and AFM results).

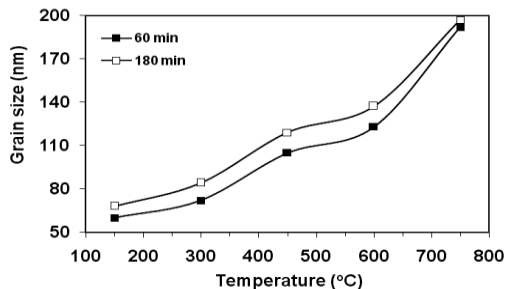


Fig. 3 – Variation of grain size of zirconium oxide thin films prepared at different times as a function of annealing temperature

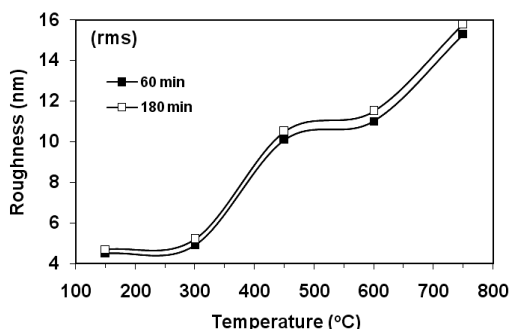


Fig. 4 – Variation of surface roughness of zirconium oxide thin films prepared at different times as a function of annealing temperature

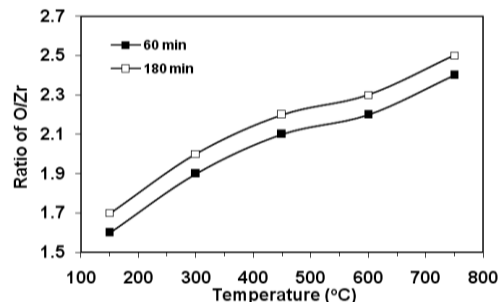


Fig. 5 – The ratio of O / Zr in zirconium oxide thin films prepared at different times as a function of annealing temperature

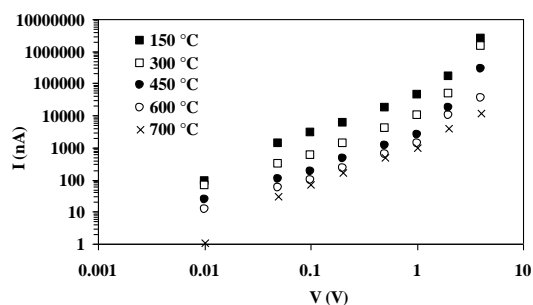
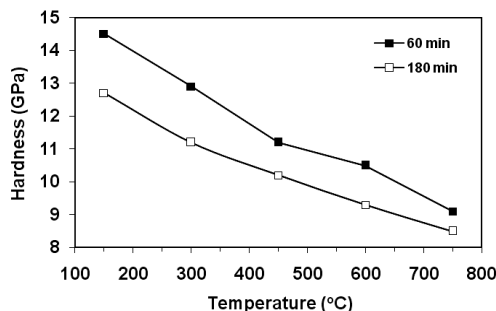


Fig. 5 – Variation of current as a function of voltage of Zr / Si thin films annealed at different temperature and time

In a polycrystalline film, grain size has a tremendous influence on the mechanical properties. Because grains usually have various crystallographic orientations, grain boundaries arise, while an undergoing deformation, slip motion will take place. Grain boundaries act as an impediment to dislocation motion for the

following two reasons: (1) dislocation must change its direction of motion due to the different orientations of grains; (2) discontinuity of slip planes from one grain to another [27]. It is also reported that film hardness and surface roughness have an inverse relation [28], so that the films with more surface roughness may possibly have an open and porous structure, which leads to lower hardness.



**Fig. 6** – Variation of hardness of zirconium oxide thin films prepared at different times as a function of annealing temperature

#### 4. CONCLUSION

Zirconium Oxide thin films prepared by post-annealing of Zr / Si (400) thin films (with 90 nm thickness) at different annealing temperatures (150-750 °C) and different annealing times (60 and 180 min) were

#### REFERENCES

1. A.N. Banerjee, K.K. Chattopadhyay, *J. Appl. Phys.* **97**, 084308 (2005).
2. A.V. Morozovska, E.A. Eliseev, *Phys. Rev. B* **73**, 104440 (2006).
3. D. Katz, T. Wizansky, O. Millo, E. Rothenberg, T. Mokari, U. Banin, *Phys. Rev. Lett.* **89**, 086801 (2002).
4. K. Khojier, H. Savaloni, *Vacuum* **84**, 770 (2010).
5. S.M. Meier, D.K. Gupta, *J. Eng. Gas Turbines Power Trans. ASME* **116**, (1994) 250.
6. W.H. Lowdermilk, D. Milam, F. Rainer, *Thin Solid Films* **73**, 155 (1980).
7. M. Copel, M. Gribelyyuk, E. Gusev, *Appl. Phys. Lett.* **76**, 436 (2000).
8. M. Houssa, V.V. Afanas'ev, A. Stesmans, M.M. Heyns, *Appl. Phys. Lett.* **77**, 1885 (2000).
9. D.K. Fork, D.B. Fenner, G.A.N. Connell, J.M. Phillips, T.H. Geballe, *Appl. Phys. Lett.* **57**, 1137 (1990).
10. J. Han, Y. Zeng, G. Xomeritakis, Y.S. Lin, *Solid State Ionics* **98**, 63 (1997).
11. M. Sayer, K. Sreenivas, *Science* **247**, 1056 (1990).
12. N.Q. Minh, *J. Am. Ceram. Soc.* **76**, 563 (1993).
13. P. Baumeister, O. Arnon, *Appl. Opt.* **16**, 439 (1977).
14. M.A. Russak, C.V. Jahnes, E.P. Katz, *J. Vac. Sci. Technol. A* **7**, 1248 (1989).
15. P.Y. Kuei, J.D. Chou, C.T. Huang, H.H. Ko, S.C. Su,

studied. Nanostructure and surface morphology of these layers were considered by XRD, AFM techniques, when the chemical composition of the films were investigated by EDAX analysis. The electrical resistance and films hardness were measured by a two probe instrument and nano-indentation test. The results showed:

I) The films annealed at 150 °C were a polycrystal of orthorhombic phase, while samples annealed at higher temperatures (300 -750 °C) showed a mixed structure of monoclinic and tetragonal.

II) Increasing of annealing temperature and time caused increasing of crystalline size, surface roughness, ratio of O / Zr in the films.

III) An increase in annealing temperature and time caused increasing of electrical resistance that was related to increasing of oxygen vacancies in films structure.

IV) The hardness of zirconium oxide thin films decreased with increasing of annealing temperature and time that were due to the increasing of grains size and surface roughness with these variables.

#### ACKNOWLEDGMENT

This work was carried out with the support of the Islamic Azad University, Chalous branch and Central Tehran Branch. The authors are grateful to Prof. H. Savaloni.

16. J. Ciosek, W. Paszkowicz, P. Pankowski, J. Firak, U. Stanislawek, Z. Patron, *Vacuum* **72**, 135 (2004).
17. A.P. Huang, P.K. Chu, *Mat. Sci. Eng.* **121**, 244 (2005).
18. L.F. Cueto, E. Sanchez, L.M. Torres-Martinez, G.A. Hirata, *Mater Charact.* **55**, 263 (2005).
19. B.J. Lee, H.L. Sohn, Y.T. Cho, *J. Korean Phys. Soc.* **51**, 1038 (2007).
20. L.D. Huy, P. Laffez, P. Daniel, A. Jouanneaux, N.T. Khoi, D. Simeone, *Mat. Sci. Eng. B: Solid.* **104**, 163 (2003).
21. J.J. Yu, I.W. Boyd, *Appl. Surf. Sci.* **208-209**, 374 (2003).
22. Y.M. Shen, S.Y. Shao, H. Yu, Z.X. Fan, H.B. He, J.D. Sha, *Appl. Surf. Sci.* **254**, 552 (2007).
23. W.C. Liu, D. Wu, A.D. Li, H.Q. Ling, Y.F. Tang, N.B. Ming, *Appl. Surf. Sci.* **191**, 181 (2002).
24. B.E. Warren, *X-ray Diffraction* (Addison Wesley Publishing Co.: London: 1969).
25. J.I. Langford, A.J. Wilson, *J. Appl. Cryst.* **11**, 102 (1978).
26. T.C. Huang, G. Lim, F. Parmigiani, E. Kay, *J. Vac. Sci. Technol. A* **3**, 2161 (1985).
27. T.G. Wang, D. Jeong, Y. Liu, Q. Wang, S. Iyengar, S. Melin, K.H. Kim, *Surf. Coat. Technol.* **206**, 2638 (2012).
28. K. Koski, J. Holsa, P. Juliet, *Surf. Coat. Technol.* **120-121**, 303 (1999).